

A POSSIBLE CORRELATION BETWEEN THE LUMINOSITIES AND LIFETIMES OF ACTIVE GALACTIC NUCLEI¹

KURT L. ADELBERGER²

Carnegie Observatories, 813 Santa Barbara Street, Pasadena, CA 91101

AND

CHARLES C. STEIDEL

Palomar Observatory, Caltech 105-24, Pasadena, CA 91125

Received 2005 March 10; accepted 2005 May 11

ABSTRACT

We use the clustering of galaxies around distant AGNs to show with $\sim 90\%$ confidence that fainter AGNs are longer lived. Our argument is simple: since the measured galaxy-AGN cross-correlation length $r_0 \sim 5 h^{-1}$ Mpc does not vary significantly over a 10 mag range in AGN optical luminosity, faint and bright AGNs must reside in dark matter halos with similar masses. The halos that host bright and faint AGNs must therefore have similar abundances, and bright AGNs are rare partly because their lifetimes are short.

Subject headings: galaxies: high-redshift — large-scale structure of universe — quasars: general

1. INTRODUCTION

In the famous paper that postulated a link between quasars and accreting black holes, Lynden-Bell (1969) remarked that the black holes created by quasar accretion would be gigantic and common, with masses around $10^8 M_\odot$ and a space density similar to that of local galaxies. It was a prescient comment, but Soltan's (1982) refinement of his calculation drew attention to the importance of the assumed quasar lifetime. The total accretion was sufficient to place a $10^6 M_\odot$ black hole inside every galaxy brighter than M31, Soltan showed, but the accreted mass might equally well be distributed among a smaller number of heavier black holes or a larger number of lighter ones. The length t_q of the quasars' lives would determine which was the case. Although the understanding of black hole formation has advanced enormously since that time, t_q remains a key parameter in theoretical models. Our ignorance of it is arguably the largest source of uncertainty in the accretion histories of supermassive black holes.

This paper is concerned not with the value of the quasar lifetime itself but rather with the idea that there is a single lifetime for accretion onto active galactic nuclei (AGNs). It is obviously an oversimplification. The duration of a luminous accretion episode is presumably affected by the mass of the central black hole, the size of the gas supply, the nature of the event that funnels gas toward the black hole, the strength and duration of dust obscuration, and so on. Our aim is to measure the extent to which this produces a systematic dependence of the lifetime on the luminosity of the AGN.

It is easy to convince oneself that such a dependence might exist. The extreme accretion associated with the most luminous QSOs is rare and must have a small duty cycle (e.g., Martini 2004), while low-level accretion has a duty cycle high enough to be observed in approximately half of all nearby galaxies (e.g., Ho 2004). As far as we know, however, no one has previously attempted a direct measurement of the dependence of AGN lifetime on luminosity (cf. Merloni 2004; Hopkins et al. 2005).

Although it may seem perverse to try to look for systematic differences in the accretion lifetime when the lifetime is still uncertain by 2 orders of magnitude (e.g., Martini 2004), in fact (as we show in § 3), changes in the lifetime are much easier to measure than the value of the lifetime itself.

Our approach exploits the well-known fact that the duty cycle of a population of objects can be inferred from its number density and clustering strength (e.g., Adelberger et al. 1998). The reason is simple. Since structure formation is hierarchical, the rarest and most massive virialized halos cluster the most strongly (e.g., Kaiser 1984), so the mass and number density of the halos that contain the objects can be deduced from the strength of the objects' clustering. The duty cycle is equal to the objects' observed number density divided by the number density of halos that can host them. If clustering measurements indicate that AGNs reside in halos of mass $10^{12} M_\odot$, for example, but the number density of AGNs is only 1% of the number density of halos with $M = 10^{12} M_\odot$, the duty cycle is evidently 0.01.

Martini & Weinberg (2001) and Haiman & Hui (2001) were the first to discuss this technique in detail. Our treatment is similar to theirs, except in one important respect: we infer the duty cycle from the clustering of galaxies around AGNs rather than from the clustering of the AGNs themselves. As pointed out by Kauffmann & Haehnelt (2002), the high number density of galaxies makes the galaxy-AGN cross-correlation length much easier to measure than the AGN autocorrelation length. A major additional benefit is that any survey deep enough to detect galaxies around bright high-redshift QSOs will inevitably detect faint AGNs at the same redshifts, increasing the sample size and the luminosity baseline over which changes in the duty cycle can be measured.

2. DATA

2.1. Galaxies

The data that we analyzed were taken from our color-selected surveys of star-forming galaxies with magnitude $R_{AB} \leq 25.5$ and redshift $1.8 \lesssim z \lesssim 3.5$. A more complete description of the surveys can be found in Steidel et al. (2003, 2004) and Adelberger et al. (2005a). We review only the most important aspects here.

The surveys consist of measured redshifts for 1627 galaxies with redshift $z > 1$ in 19 fields scattered around the sky (Table 1).

¹ Based, in part, on data obtained at the W. M. Keck Observatory, which is operated as a scientific partnership between the California Institute of Technology, the University of California, and NASA, and was made possible by the generous financial support of the W. M. Keck Foundation.

² Carnegie Fellow.

TABLE 1
OBSERVED FIELDS

Field	α (J2000.0)	δ (J2000.0)	N_{gal}^a	$N_{\text{AGN}}^{>-24b}$	$N_{\text{AGN}}^{<-24c}$
B20902+34.....	09 05 31	34 08 02	31	1	0
CDFb.....	00 53 42	12 25 11	19	1	0
DSF 2237a.....	22 40 08	11 52 41	41	1	0
DSF 2237b.....	22 39 34	11 51 39	43	2	1
HDF.....	12 36 51	62 13 14	251	5	1
Q0000-263 ^d	00 03 23	-26 03 17	15	2	0
PKS 0201+113.....	02 03 47	11 34 45	23	1	1
LBQS 0256-0000.....	02 59 06	00 11 22	45	2	1
LBQS 0302-0019.....	03 04 50	00 08 13	42	1	1
FBQS J0933+2845.....	09 33 37	28 45 32	63	1	1
Q1305.....	13 07 45	29 12 51	76	4	3
Q1422+2309.....	14 24 38	22 56 01	108	5	1
Q1623.....	16 25 45	26 47 23	200	9	7
HS 1700+6416.....	17 01 01	64 12 09	88	1	1
Q2233+136.....	22 36 27	13 57 13	43	3	1
Q2343+125.....	23 46 05	12 49 12	188	2	4
Q2346.....	23 48 23	00 27 15	44	3	3
SSA 22a.....	22 17 34	00 15 04	59	0	2
WESTPHAL.....	14 17 43	52 28 48	248	7	0
Total.....			1627	51	28

NOTE.—Units of right ascension are hours, minutes, and seconds, and units of declination are degrees, arcminutes, and arcseconds.

^a Number of (nonactive) galaxies with spectroscopic redshift $z > 1$.

^b Number of AGNs with spectroscopic redshift $z > 1$ and rest-frame 1350 Å absolute AB magnitude $M_{1350} > -24$.

^c Number of AGNs with spectroscopic redshift $z > 1$ and $M_{1350} \leq -24$.

^d The field is centered on this QSO, but the QSO itself is excluded from our analysis because we lack a good spectrum.

(These totals exclude any survey fields with no detected AGNs and include only the galaxies with the most certain redshifts.) The size of the fields varies but is typically ~ 100 – 200 arcmin². The coordinates of some fields were chosen more or less at random, but most fields were centered on a bright QSO or group of QSOs. Objects were selected for spectroscopy if their U_nGR colors indicated that they were likely to lie in the targeted range of redshifts. Our decision to obtain a spectrum of an object was influenced only by its U_nGR colors, R magnitude, and spatial position; we were more likely to observe objects if they had $23 < R < 24.5$, if they had colors similar to those expected for AGNs, or if they lay close to a known AGN, and we rarely observed objects whose colors did not satisfy the selection criteria of Steidel et al. (2003) and Adelberger et al. (2004). The overall redshift distribution of the galaxies in these fields is shown in Figure 1. Their distribution of absolute magnitudes, calculated from observed broadband colors for a concordance cosmology with $\Omega_m = 0.3$, $\Omega_\Lambda = 0.7$, and $h = 0.7$, is shown in Figure 2.

2.2. AGNs

Fifty-seven of the 1684 objects in our spectroscopic sample have strong emission in both Ly α and C IV $\lambda 1549$. We classify these objects as AGNs for reasons that are discussed in Steidel et al. (2002). Although some of our faintest AGNs might be misclassified as galaxies because their C IV lines are too weak for us to detect, the lack of C IV emission in the thousand-object composite spectrum of Shapley et al. (2003) shows that these misclassified AGNs must be rare.

Our total sample of AGNs was increased to 79 by adding the previously known AGNs that we deliberately included in our survey fields. Since C IV was the only line (aside from Ly α) detected with reasonable significance in every AGN spectrum, we

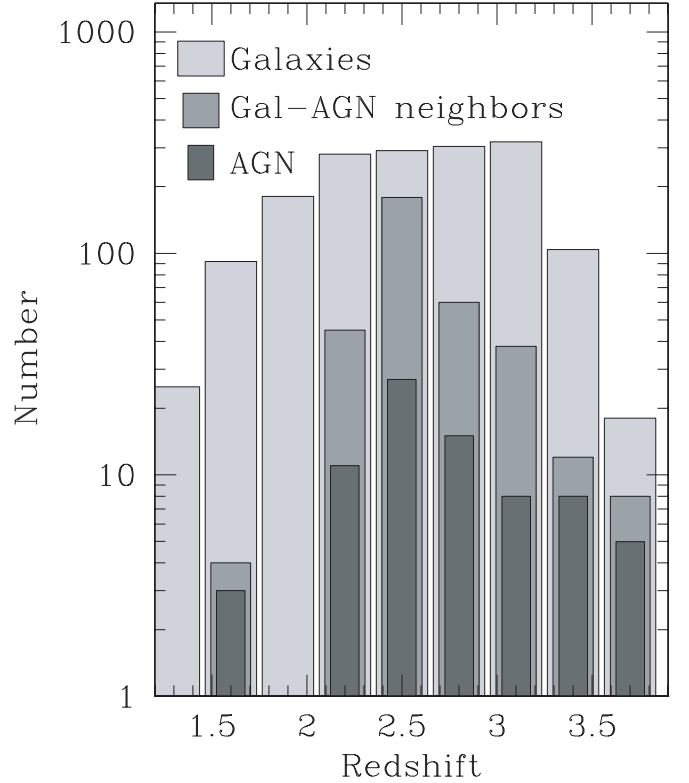


FIG. 1.—Redshift distributions for the galaxies and AGNs in our sample. Also shown are the number of galaxy-AGN neighbors, defined as the number of galaxy-AGN pairs with angular separation $60'' < \theta < 300''$ ($1.2 h^{-1}$ comoving Mpc $\lesssim R \lesssim 6.2 h^{-1}$ comoving Mpc) and radial separation $\Delta Z < 30 h^{-1}$ comoving Mpc.

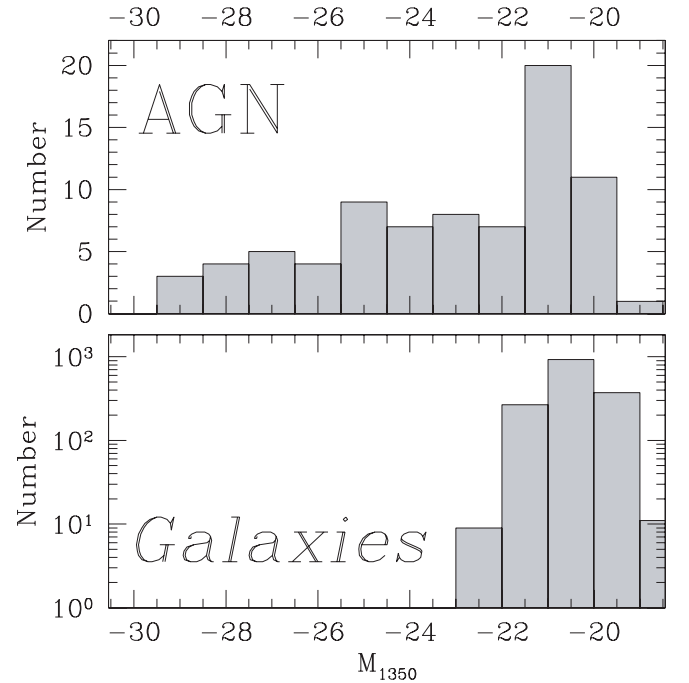


FIG. 2.—Distribution of absolute AB magnitudes at rest-frame 1350 Å for the AGNs and galaxies in our spectroscopic sample. No corrections for incompleteness have been applied, so these do not resemble the true distributions for the underlying populations.

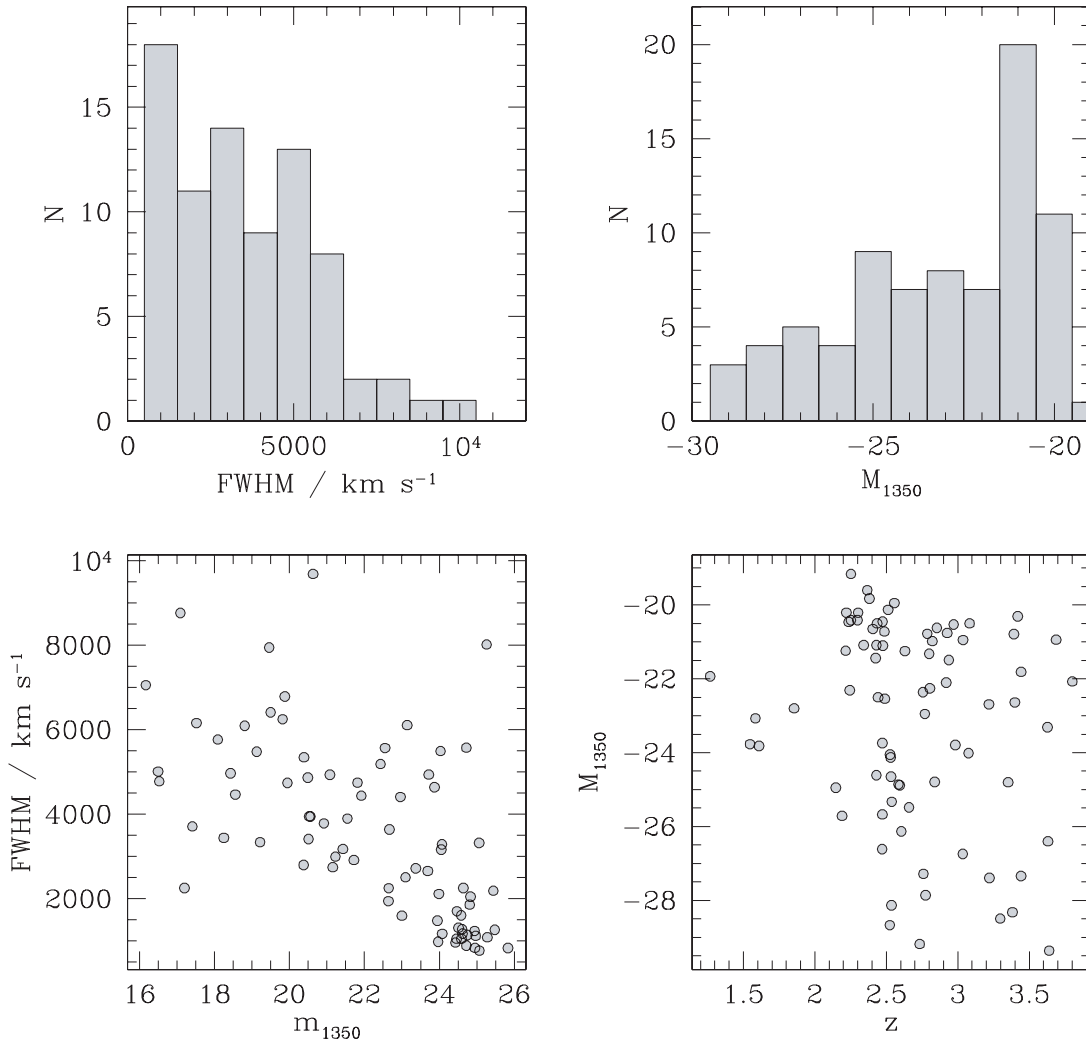


FIG. 3.—Overview of the characteristics of the AGNs in our sample. *Top left*: Histogram of C IV line width. The typical uncertainty ranges from 10% to 20% and is dominated by systematic errors (e.g., continuum placement) for the brightest AGNs. *Top right*: Histogram of absolute AB magnitude at rest-frame 1350 Å (M_{1350}). The uncertainty in the AB magnitude is $\lesssim 0.2$ mag for even our faintest objects (e.g., Steidel et al. 2003). *Bottom left*: Relationship between C IV line width and apparent AB magnitude at rest-frame 1350 Å. *Bottom right*: M_{1350} against redshift. Recall that the selection bias is severe in our AGN sample, since (for example) we deliberately targeted AGNs that were bright and had broad emission lines. These panels show the characteristics of our sample as selected, not of a fair sample of high-redshift AGNs.

based our redshift assignments on it. In their analysis of 3814 QSOs from the Sloan Digital Sky Survey, Richards et al. (2002) found that C IV was blueshifted on average by 824 km s^{-1} compared to Mg II, which they assumed was at the QSO’s systemic redshift. We accordingly assumed that the true redshift of each of our AGNs was 824 km s^{-1} redder than the peak of C IV emission. Since Richards et al. (2002) report a scatter in the C IV–Mg II velocity offsets of 500 km s^{-1} , we expect that the uncertainty in our QSO redshifts will be approximately 500 km s^{-1} . Although the way we assign redshifts is better suited to our sample’s broad-lined AGNs, any mistakes in the redshifts of narrow-lined AGNs are unlikely to affect our conclusions: as we will see, the typical redshift error would have to be $\sim 3000 \text{ km s}^{-1}$ (i.e., $\sim 30 h^{-1}$ comoving Mpc) to alter our clustering measurements significantly. Figure 1 shows the redshift distribution for the 79 AGNs. Figure 3 shows their distribution of velocity FWHM and apparent magnitude.

Strong emission lines prevented us from calculating AB magnitudes of the AGNs at rest-frame 1350 Å directly from their broadband magnitudes. Instead, we scaled each AGN spectrum to match its observed G and R magnitudes, measured the flux density near 1350 Å, then converted to absolute magnitude for a cosmology with $\Omega_m = 0.3$, $\Omega_\Lambda = 0.7$, and $h = 0.7$. This pro-

cedure failed for our brightest sources, those with $G \lesssim 18$, which were saturated in our images. For these we adopted the magnitude implied by their unscaled flux-calibrated spectra. Three of our sources were saturated and lacked flux-calibrated spectra. The magnitudes of these were taken from the Sloan Digital Sky Survey archive or from photographic measurements in the NASA/IPAC Extragalactic Database. Figure 2 shows the resulting histogram of AGN absolute magnitudes. Although unintended, our selection strategy has given us a sample of AGNs with brightnesses distributed almost uniformly over a 10 mag range. Comparison to the galaxies’ apparent magnitude distribution suggests that stellar light may contribute significantly to the measured magnitudes of the faintest AGNs. We do not correct for this. Doing so would only strengthen our conclusions, since the faintest AGNs would be even fainter than we assume.

2.3. Simulations

In a number of places our interpretation of the data relies on the GIF- Λ CDM numerical simulation of structure formation in a cosmology with $\Omega_m = 0.3$, $\Omega_\Lambda = 0.7$, $h = 0.7$, $\Gamma = 0.21$, and $\sigma_8 = 0.9$. This gravity-only simulation contained 256^3 particles with mass $1.4 \times 10^{10} h^{-1} M_\odot$ in a periodic cube of comoving side length $141.3 h^{-1} \text{ Mpc}$, used a softening length of $20 h^{-1}$

comoving kpc, and was released publicly, along with its halo catalogs, by Frenk et al. (2000). Further details can be found in Jenkins et al. (1998) and Kauffmann et al. (1999). Although the simulation does not include much of the physics associated with galaxy formation, we make use only of its predictions for the statistical distribution of dark matter on large (≥ 1 Mpc) scales. Since the GIF- Λ CDM cosmology is consistent with the *Wilkinson Microwave Anisotropy Probe* results (Spergel et al. 2003) and since modeling the gravitational growth of perturbations on large scales is not numerically challenging, the large-scale distribution of dark matter in this simulation should closely mirror that in the actual universe.

3. METHODS

3.1. Estimating r_0

We estimated the correlation lengths of the samples with two approaches. Both correct for the irregular angular sampling of our spectroscopy and are unaffected by the selection criteria that were used to include AGNs in our sample. The second approach is also insensitive to the criteria that were used to select the galaxies. See Adelberger (2005) for a more complete discussion.

In the first approach, we cycle through the AGNs in our sample, calculating for each one both the number $N_{\text{obs}}(l)$ of galaxies in the AGN field whose comoving radial separation from the AGN ΔZ is less than $l = 30 h^{-1}$ Mpc and the number $N_{\text{exp}}(l, r_0)$ that would be expected if the correlation function had the form $\xi(r) = (r/r_0)^{-1.6}$. The quantity $N_{\text{exp}}(l, r_0)$ is related straightforwardly to the integral of the correlation function along the lines of sight to galaxies in the field. As shown by Adelberger (2005),

$$N_{\text{exp}}(l, r_0) = \sum_j^{\text{galaxies}} \frac{\int_{z_i - \Delta z}^{z_i + \Delta z} dz P_j(z) [1 + \xi(r_{ij})]}{\int_0^\infty dz P_j(z) [1 + \xi(r_{ij})]}, \quad (1)$$

where the sum runs over all galaxies in the AGN's field, z_i is the AGN redshift, Δz is the redshift difference corresponding to a comoving radial separation of size l , $P_j(z)$ is the selection function for the j th galaxy,³ normalized so that $\int_0^\infty dz P_j(z) = 1$, and r_{ij} is the distance between the AGN and a point at redshift z with the galaxy's angular separation θ_j . We then sum the values $N_{\text{obs}}(l)$ and $N_{\text{exp}}(l, r_0)$ for all our AGNs and take as our best-fit correlation length the value of r_0 that makes the total expected neighbor counts equal to the total observed. To ensure that our estimate of r_0 reflects the clustering strength on large (≥ 1 Mpc) scales rather than conditions inside the AGN halos, we exclude from consideration any galaxy-AGN pairs with angular separation $\theta < 60''$ (i.e., $1.2 h^{-1}$ comoving Mpc at $z = 2.5$). Galaxy-AGN pairs with $\theta > 300''$ are also excluded, since the weak clustering signal at the largest angular separations can be overwhelmed by low-level systematic errors (Adelberger 2005).

The approach of the preceding paragraph can fail if the assumed selection functions P_j are inaccurate. To guard against this possibility, we also estimate r_0 by finding the value that makes

$$\frac{\sum_{\text{AGN}} N_{\text{obs}}(l)}{\sum_{\text{AGN}} N_{\text{obs}}(2l)} = \frac{\sum_{\text{AGN}} N_{\text{exp}}(l, r_0)}{\sum_{\text{AGN}} N_{\text{exp}}(2l, r_0)}. \quad (2)$$

³ Since the galaxies in our samples were chosen with different color-selection criteria, their expected redshift distributions are different. In this approach, we set P_j to the observed LBG redshift distribution if the object was selected with the LBG selection criteria and to the observed BX redshift distribution if the object was selected with the BX criteria. Otherwise, the galaxy is ignored. (See Adelberger et al. [2004] for a definition of these criteria and plots of their redshift distributions.)

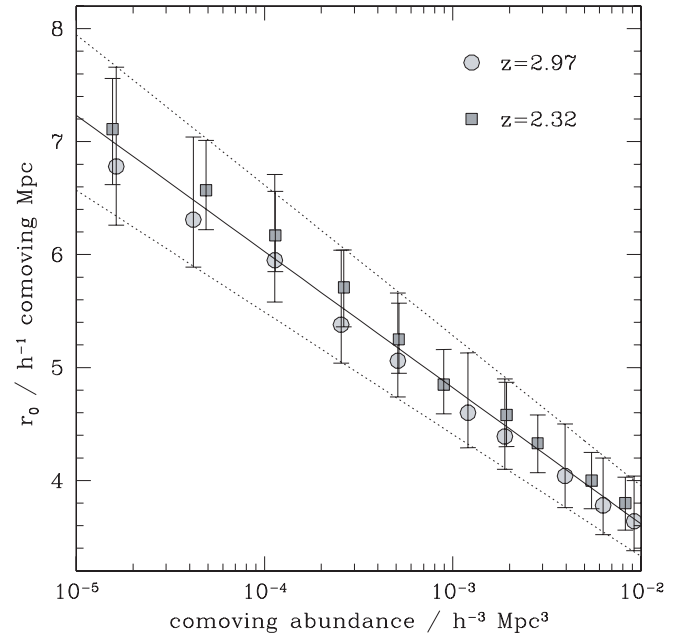


FIG. 4.—Theoretical relationship between the cross-correlation length r_0 and the AGN-halo comoving abundance n . Points show the GIF- Λ CDM relationship at two redshifts. The error bars indicate the uncertainty in the relationship due to the uncertainty in the galaxies' threshold mass. The solid line shows the least-squares compromise that we adopt throughout: $\log [n/(h^{-1} \text{ Mpc})^3] = -0.83r_0 + 1.00$. The upper and lower dotted lines show the relationships that would result if we altered the assumed threshold mass by $\pm 1 \sigma$. Fig. 6 shows that our conclusions would not be significantly affected if we adopted these relationships instead.

Taking the ratio causes most systematic errors to cancel (Adelberger 2005). Since it also increases the random errors, however, we use equation (2) only to verify that systematic errors have not badly compromised the estimate of r_0 obtained from the first approach.

3.2. Estimating the Duty Cycle

As stated in the introduction, our definition of duty cycle is the observed number density of AGNs divided by the number density of halos that can host them. Calculating it requires two steps.

3.2.1. Halo Abundance

We use the GIF- Λ CDM simulations to estimate the halo abundance from r_0 . For each of the publicly released catalogs⁴ of halos at redshifts $2 < z < 3$, we calculated the cross-correlation function $\xi_{M_1, M_2}(r)$ of halos in two mass ranges, $M > M_1$ and $M > M_2$, for different choices of M_1 and M_2 and estimated the cross-correlation length r_0 by fitting a power law to ξ_{M_1, M_2} at separations $1 h^{-1} \text{ Mpc} < r < 10 h^{-1} \text{ Mpc}$. After calculating the number density of halos with $M > M_2$ in the simulations at redshift z , we stored our results as a table $r_0(z, M_1, n_2)$, giving the expected cross-correlation length at redshift z between halos with mass threshold M_1 and halos with number density n_2 . If all our observations were at redshift z_0 and we knew the threshold mass M_g of the galaxies' halos, we could convert any measured correlation length r_0 into a number density n_q of AGN halos by simply looking up the value of n_q that made the tabulated $r_0(z_0, M_g, n_q)$ equal our observed correlation length. In fact, our observations are at a range of redshifts, and the galaxy mass is not precisely known. Figure 4 shows the uncertainty in the relationship between r_0 and n_q that results from the range of redshifts in our survey and from the 1σ uncertainty in the galaxy masses

⁴ That is, for the catalogs at $z = 2.97, 2.74, 2.52, 2.32$, and 2.12 .

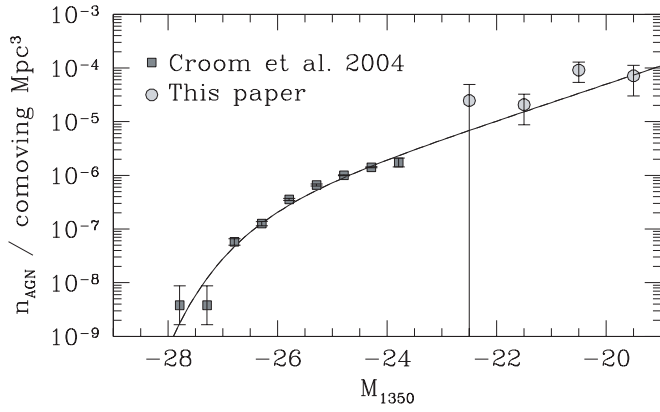


FIG. 5.—Observed number density vs. magnitude for AGNs at $z \sim 2$. Squares show the 2dF QSO luminosity function of Croom et al. (2004). Circles show our rough estimate of the AGN luminosity function at fainter magnitudes, calculated from our survey with the method described in § 3.2.2. The crude completeness corrections of this approach yield a luminosity function adequate only for cases like ours for which low accuracy is tolerable. The parameters of the Schechter function (solid line; $M_* = -26.2$, $\alpha = -1.85$, and $\Phi_* = 4 \times 10^{-7} \text{ Mpc}^{-3}$) should not be used in other situations.

(Adelberger et al. 2005b). For the remainder of the paper we adopt an r_0 - n_q relationship that is a least-squares fit to the data in the figure (Fig. 4, solid line). Although we can offer little justification for this compromise, the exact choice of relationship has almost no effect on our conclusions. Any errors in the relationship increase or decrease in tandem the implied duty cycles for bright and faint AGNs; they alter the absolute value that we infer for the duty cycles but not the relative difference between them. (We demonstrate that this is true in Fig. 6.) This is one of the main strengths of our approach. It justifies our claim in § 1 that a systematic variation of AGN lifetime with luminosity is easier to measure than the absolute value of the lifetime itself.

3.2.2. AGN Abundance

We adopt a crude approach since small (tens of percent) errors in the AGN abundance have little effect on our conclusions. At the faintest magnitudes we estimate the AGN number density by multiplying the galaxy luminosity function at $z = 3$ (Adelberger & Steidel 2000) by $f(M_{1350})$, the fraction of sources in our spectroscopic sample with absolute magnitude M_{1350} that were observed to be AGNs. Note that we are including all AGNs in this analysis, not merely the broad-lined AGNs considered by Hunt et al. (2004). Since the faint end of the rest-frame UV luminosity distribution of galaxies does not evolve significantly from $z = 3$ to 2 (N. A. Reddy et al. 2005, in preparation), this number density should be roughly appropriate down to $z = 2$. At the brightest magnitudes we adopt the Two-Degree Field (2dF) $1.81 < z < 2.10$ QSO luminosity function of Croom et al. (2004).⁵ The AGN luminosity distribution is fit tolerably well by a Schechter function (Fig. 5), and we use this fit to estimate the number density of AGNs in each range of apparent magnitude.

4. RESULTS

The first approach of § 3.1 leads to the estimates $r_0 = 4.7$ and $5.4 h^{-1}$ comoving Mpc for the galaxy-AGN cross-correlation

⁵ We convert the absolute magnitudes M_b , reported by Croom et al. (2004) to M_{1350} by adding 0.46 mag; subtracting 0.07 mag converts to the AB system, and adding 0.53 mag undoes their K -correction from observed-frame to rest-frame b_j (Cristiani & Vio 1990).

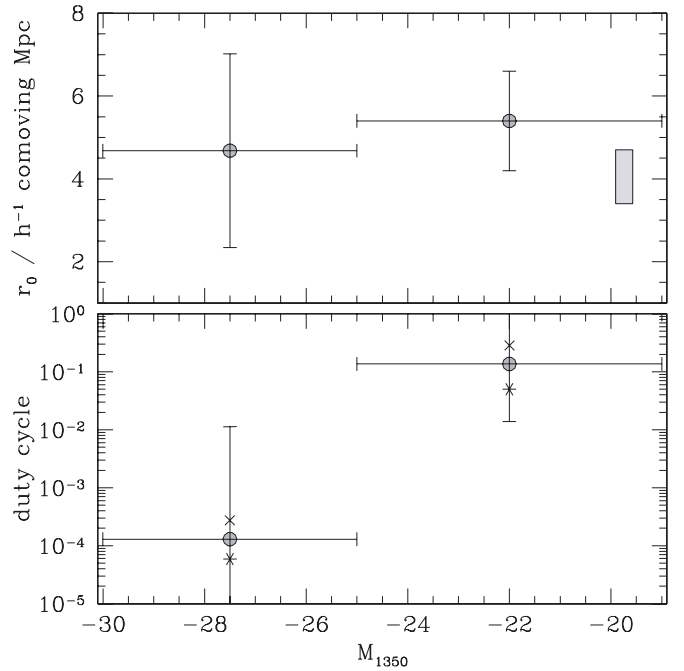


FIG. 6.—*Top*: Galaxy-AGN cross-correlation length as a function of AGN luminosity M_{1350} . Points with error bars show our measurements. The shaded rectangle shows the $\pm 1 \sigma$ range of the galaxy-galaxy correlation length at similar redshifts (Adelberger et al. 2005a); its abscissa is arbitrary. *Bottom*: Implied duty cycle as a function of AGN luminosity. Error bars show the $\pm 1 \sigma$ random uncertainty. The four- and six-pointed stars show how our estimated duty cycle would change if we altered the assumed relationship between clustering strength and abundance by an amount similar to its uncertainty. (They correspond to the upper and lower dotted envelopes in Fig. 4.) Note that the confidence intervals shown in this plot reflect only the constraints from our clustering analysis. Other considerations rule out a duty cycle of ≥ 1 for the faint AGNs and $\leq 10^{-5}$ for the bright AGNs, however. See § 5 for further discussion.

length of AGNs with magnitude $-30 < M_{1350} < -25$ and $-25 < M_{1350} < -19$, respectively. An easy way to estimate the uncertainty is suggested by the similarity of the cross-correlation length to the galaxy-galaxy correlation length reported by Adelberger et al. (2005b): generate many alternate realizations of the data by treating randomly chosen galaxies in each field as that field's AGNs, rather than the true AGNs themselves, and recalculate r_0 for each simulated sample. The rms dispersion of r_0 among these simulated samples should be roughly equal to the uncertainty in r_0 . We adopted it for the error bars in Figure 6 (top). The true uncertainty is likely to be somewhat smaller, since our spectroscopic selection strategy gave our AGNs more angular neighbors with measured redshifts than the typical galaxy.

Figure 6 (bottom) shows the same data, except the cross-correlation length has been converted to a duty cycle with the approach of § 3.2. As emphasized in that section, uncertainties in the r_0 -abundance relationship mean that the labels on the y -axis could be wrong by a multiplicative constant, but relative differences in the duty cycle should be secure.

To estimate the significance of the apparent difference in duty cycle, we note that our adopted relationship between r_0 and the halo number density implies that r_0 would be $2.92 h^{-1}$ comoving Mpc larger for AGNs with $-30 < M_{1350} < -25$ than for AGNs with $-25 < M_{1350} < -19$ under the null hypothesis that the duty cycle is independent of M_{1350} . The observed difference in best-fit correlation length, $-0.72 h^{-1}$ comoving Mpc, is therefore $3.64 h^{-1}$ comoving Mpc smaller than the difference that would

be expected under the null hypothesis. A difference as large or larger than $\Delta r_0 = 3.64 h^{-1}$ Mpc between AGNs with $-25 < M_{1350} < -19$ and $-30 < M_{1350} < -25$ occurred in 10% of the randomized AGN samples described above. We conclude that the null hypothesis of a constant duty cycle can be rejected with roughly 90% confidence.

5. SUMMARY AND DISCUSSION

We measured the galaxy-AGN cross-correlation length r_0 as a function of the AGN luminosity. The comoving cross-correlation length was similar for bright and faint AGNs, $r_0 = 4.7 \pm 2.3 h^{-1}$ Mpc for $-30 < M_{1350} < -25$ and $r_0 = 5.4 \pm 1.2 h^{-1}$ Mpc for $-25 < M_{1350} < -19$, which led us to conclude with 90% confidence that both are found in halos with similar masses and that bright AGNs are rarer because their duty cycle is shorter. Since halo lifetimes depend only weakly on halo mass (e.g., Martini & Weinberg 2001), the difference in duty cycle implies that optically faint AGNs have longer lifetimes.

Our analysis differs from previous work (e.g., that of Croom et al. [2005], who also found no luminosity dependence in the AGN clustering strength) in two principal ways. We estimated the duty cycle from the cross-correlation of galaxies and AGNs, not from the autocorrelation function of AGNs, and our sample included AGNs with a much wider range of luminosities, extending ~ 4 mag fainter than the QSO threshold $M_{1350} = -23$. These differences allowed us to obtain our measurement from a comparatively small survey. An appraisal of this result should cover at least the following three points.

The first is obvious: it is only marginally significant. Larger samples are required to prove that the duty cycle depends on luminosity. Moreover, other arguments suggest that the minimum allowed duty cycle at high luminosity should be increased and that the maximum allowed at low luminosity should be decreased. Since the AGN lifetime is roughly the age of the universe times the duty cycle (e.g., Martini & Weinberg 2001), a duty cycle of $\lesssim 10^{-5}$ for the brightest AGNs is incompatible with the observed proximity effect in QSO spectra (e.g., Martini 2004) and with the lack of flickering QSOs in the Sloan Digital Sky Survey (Martini & Schneider 2003). A duty cycle of roughly unity for the fainter AGNs is implausible as well, since a black hole radiating continuously would almost certainly be too faint compared to its galaxy for us to detect: the difference in energetic efficiency for black hole accretion ($0.1mc^2$) and hydrogen burning ($0.007mc^2$) implies that a galaxy's steadily radiating black hole would be much fainter than its stars if the final ratio of black hole to stel-

lar mass is $M_{\text{BH}}/M_* \sim 0.001$.⁶ Taking these arguments into account would bring the high- and low-luminosity duty cycles closer together in Figure 6.

Second, the physical interpretation is not straightforward. Recall that we have defined the duty cycle for the absolute magnitude range $M_{\text{lo}} < M < M_{\text{hi}}$ as the ratio of the number density of AGNs with those magnitudes to the number density of halos that can host them. In the Appendix we show that this duty cycle would be independent of magnitude if black holes accreted only at the Eddington rate, were not obscured by dust, and had masses that followed a tight power-law correlation with the total masses M_h of galaxies that contain them. The duty cycle would decrease at large luminosities if brighter AGNs were more heavily obscured, if black hole masses fell below the predictions of the $M_{\text{BH}}-M_h$ correlation at very large M_h , or if anything (e.g., complicated light curves) caused a broad range of luminosities L in the AGNs that lie within halos of a given mass M_h . Each of these is expected theoretically (e.g., Hopkins et al. 2005). The apparent decrease of the duty cycle at large luminosities presumably results from a combination of physical effects, and our observations do not identify which is dominant among them.

Finally, our result was derived from a small survey designed for other purposes. Most of the brightest AGNs lay behind the survey galaxies, not in their midst, reducing the number of galaxy-AGN pairs and increasing the uncertainty in r_0 . A large, optimized survey could easily shrink the error bars severalfold. The only useful contribution of this paper may be the demonstration that a definitive measurement is within easy reach.

K. L. A. would like to thank L. Ho, L. Hernquist, L. Ferrarese, and J. Kollmeier for many interesting conversations and an anonymous referee for encouraging us to discuss the physical interpretation of the duty cycle. Our collaborators in the Lyman break survey did most of the work in taking and reducing these data. We are grateful that they let us proceed with the analysis. This research has made use of the NASA/IPAC Extragalactic Database (NED), which is operated by the Jet Propulsion Laboratory, California Institute of Technology, under contract with the National Aeronautics and Space Administration.

⁶ Note that the lack of a detected AGN in most high-redshift galaxies is not by itself an argument against a duty cycle of unity for AGNs with luminosities $-25 < M_{1350} < -19$. These AGNs could shine exclusively within the most massive galaxies, leaving the less massive galaxies with AGNs that are undetectably faint.

APPENDIX

PHYSICAL INTERPRETATION OF THE DUTY CYCLE

We discuss three simple models for AGN evolution that may help illustrate the physical meaning of the duty cycle. Suppose first that the black hole mass M_{BH} is tightly correlated with the total galaxy mass M_h at all times, that the correlation has the form $M_{\text{BH}} \propto M_h^\alpha$, that AGNs are unobscured by dust, and that black holes radiate either at the Eddington rate $L_{\text{Edd}}(M_{\text{BH}})$ or not at all, gaining their mass in a few short accretion episodes separated by long periods of quiescence. The duty cycle would then be independent of the AGN magnitude, as can be seen with the following argument.

Begin by considering the evolution of a black hole inside a single dark matter halo of given mass M_h . When the halo forms in the very early stages of a merger of two smaller halos, its black hole mass⁷ may initially be smaller than the mean mass implied by the $M_{\text{BH}}-M_h$ correlation, but by the time the halo is destroyed by mergers, roughly 1 Hubble time later (Martini & Weinberg 2001), the black hole

⁷ This black hole mass may initially be divided among two black holes; since the Eddington luminosity of a black hole of mass $2M$ is equal to the sum of the Eddington luminosities of two black holes each of mass M , this does not affect our argument.

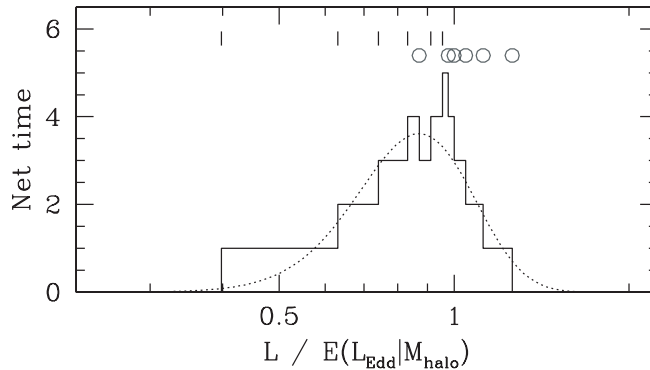


FIG. 7.—Net time spent at a given luminosity for an ensemble of six black holes in the first toy model considered in the Appendix. We assume that these black holes radiate at the Eddington luminosity and lie inside six halos of equal mass M_h . If the black holes have the initial luminosities that are marked with vertical lines and they grow until the luminosities have reached the final values marked with circles, then the total amount of time that the six AGNs spent radiating at a given luminosity is shown by the histogram. The distribution for *all* AGNs in halos of mass M_h , not just these six AGNs, might look more like the dotted curve in the background. If the black hole and the halo mass are tightly correlated and all accretion is at the Eddington rate, this function has to be narrow. The units on the x -axis are normalized to $E(L_{\text{Edd}}|M_h)$, the mean Eddington luminosity of all AGNs in halos of mass M_h ; units on the y -axis are arbitrary.

must have grown enough to fall on the correlation. Otherwise, the correlation could not be satisfied by the ensemble of all halos. Since accretion at the Eddington rate produces exponential growth, the black hole spends equal amounts of time in each octave of luminosity as it grows from its initial mass M_i to its final mass M_f ; if one were to plot the amount of time spent in each logarithmic interval of luminosity L , it would be constant for $L_{\text{Edd}}(M_i) < L < L_{\text{Edd}}(M_f)$ and 0 elsewhere. This is equally true if the growth occurs in many discrete episodes of accretion or in a single burst. Now consider a plot of total elapsed time versus luminosity for the black holes within N randomly chosen halos of the same mass M_h . The plot would be the superposition of N boxcars with random left and right edges, producing an overall shape that is peaked near the Eddington luminosity of the typical black hole associated with halos of mass M_h . Figure 7 shows an example for $N = 6$. The same plot for the ensemble of all halos of mass M_h would be a smoother realization of a similar function. Call this plot the kernel. Since the number of AGNs we observe with a given luminosity is proportional to the net time that AGNs spend at that luminosity, the kernel is the AGN luminosity distribution that we would observe if the universe consisted solely of halos with mass M_h . The width of the kernel depends on how far the initial and final black hole masses stray from the expectation value $E(M_{\text{BH}}|M_h)$, but it must be very narrow compared to the multidecade width of the halo mass distribution. Otherwise, our assumption of a tight $M_{\text{BH}}-M_h$ correlation would be violated. The AGNs within a narrow range of luminosity therefore must lie inside halos with a narrow range of masses. Our definition of duty cycle for $L_{\text{min}} < L < L_{\text{max}}$ is the number density of AGNs within that range of luminosity divided by the number density of halos that can host them. In this scenario, it is equal to the time required for the AGN's luminosity to grow from L_{min} to L_{max} if it is accreting at the Eddington rate divided by the halos' mean lifetime. The numerator is independent of halo mass for logarithmic luminosity intervals, and the denominator depends extremely weakly on halo mass (Martini & Weinberg 2001). Therefore, the duty cycle in logarithmic luminosity bins should be nearly independent of halo mass or AGN luminosity.

To check this claim, we generated an ensemble of simulated AGNs by starting with an ensemble of halos following a Press-Schechter mass function ($\Omega_m = 0.3$, $\Omega_\Lambda = 0.7$, $\Gamma = 0.2$, and $\sigma_8 = 0.9$, $z = 2.5$), assigning each halo an expected central black hole mass with the relationship $M_{\text{BH}} = 10^7 (M_h/10^{12} M_\odot)^{1.65}$ (Ferrarese 2002) and giving each black hole a luminosity equal to the Eddington luminosity of the expected mass times a number drawn at random from the kernel (Fig. 7). This resulted in the AGN luminosity distribution shown in Figure 8 (*top left*). The distribution of halo masses for AGNs with luminosities $L_{\text{Edd}}(10^6 M_\odot) < L < L_{\text{Edd}}(10^8 M_\odot)$ and $L_{\text{Edd}}(10^8 M_\odot) < L < L_{\text{Edd}}(10^{10} M_\odot)$ is shown in Figure 8 (*middle left*). Figure 8 (*bottom left*) shows the inferred duty cycle in these luminosity ranges, i.e., the ratio of AGN number density in each luminosity range to the number density of halos more massive than the mean associated halo mass shown in Figure 8 (*middle left*). This is roughly the duty cycle that would be estimated with the approach that we adopted above. It is the same for the two logarithmic luminosity ranges, as expected.

The scenario can be altered in two ways to make the duty cycle decrease at larger luminosities. The first is to increase the number density of halos that can host the brightest AGNs. For a fixed halo mass distribution, this can be accomplished by relaxing our assumption that accretion occurs only at the Eddington rate or by increasing the scatter in the $M_{\text{BH}}-M_h$ relationship. Either increases the scatter in the relationship between M_h and L , raising the probability that a high-luminosity AGN resides within a low-mass halo. Figure 8 (*middle column*) shows one example of how a broad distribution of L at fixed M_h makes the duty cycle depend on luminosity.

The second way is to reduce the lifetimes of the brightest AGNs. If the $M_{\text{BH}}-M_h$ correlation is a tight power law and all accretion is at the Eddington rate, then we can adjust neither the mean accreted mass for black holes in the most massive halos nor the rate at which accretion occurs. In this case the optical lifetimes of the brightest AGNs can be reduced only by making them heavily obscured while they accrete most of their mass. The lifetimes can also be reduced, even for unobscured Eddington-rate accretion, if we change the form of the $M_{\text{BH}}-M_h$ relationship. One change seems well motivated: letting the relationship break down for halos with supergalactic masses. Ferrarese's (2002) relationship $M_{\text{BH}} \sim 10^7 (M_h/10^{12} M_\odot)^{1.65} M_\odot$ predicts that local clusters of mass $10^{15} M_\odot$ should contain $10^{12} M_\odot$ central black holes, for example, but there is no evidence that these ultramassive black holes exist. It seems more likely that black hole formation becomes as suppressed as star formation in halos with mass $M_h \gg 10^{13} M_\odot$. Suppressing or obscuring the brightest AGNs can make the duty cycle depend strongly on luminosity, as Figure 8 shows.

If additional observations confirm the decrease in duty cycle at high luminosities, some combination of these effects would presumably be responsible.

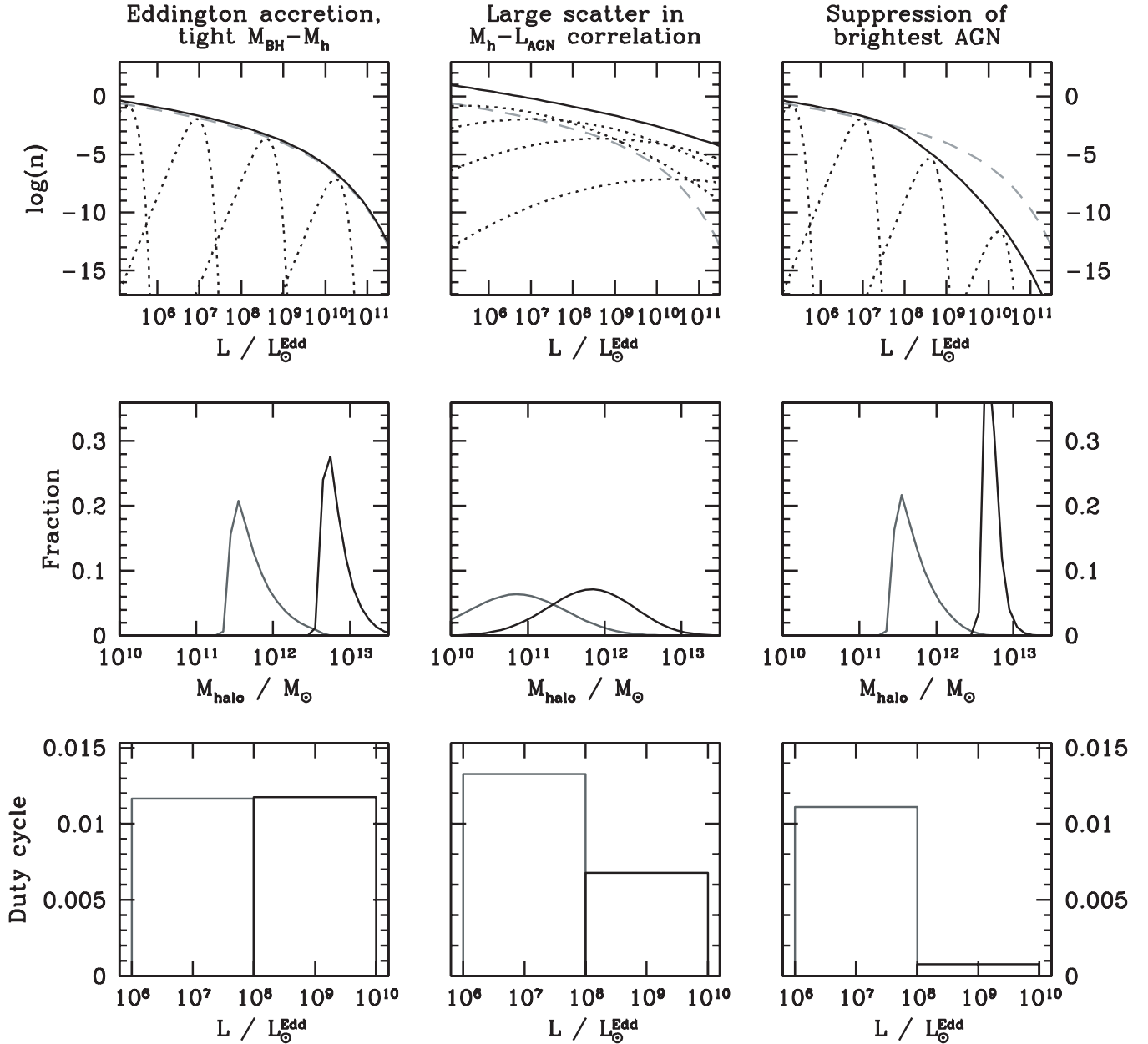


FIG. 8.—Dependence of duty cycle on luminosity for three toy models. We generated an ensemble of simulated central black holes from a Press-Schechter mass function by associating each halo of mass M_h with a black hole of expected mass $M_{\text{BH}}/M_{\odot} = 10^7(M_h/10^{12} M_{\odot})^{1.65}$ (Ferrarese 2002), then associated each black hole with a luminosity obtained under different assumptions for the three models. Each column shows results for one model. The left panels assume Eddington accretion and a tight correlation of M_h and M_{BH} . The middle panels assume large scatter in the relationship between M_h and AGN luminosity L . The right panels assume Eddington accretion but stunt the growth of black holes in the most massive halos. Units on the y -axis are arbitrary in all panels. *Top*: Dashed lines show the luminosity distribution that would have resulted if each black hole had exactly the mean mass predicted by the $M_{\text{BH}}-M_h$ relationship and radiated at its Eddington luminosity. Instead, we assume that each halo's AGN luminosity has some scatter around its expectation value. Dotted lines indicate the assumed luminosity distribution for halos of mass 10^{12} , 10^{13} , 10^{14} , and $10^{15} M_{\odot}$. They show the assumed scatter in the M_h-L relationship, which is large for the middle model and equally small for the left and right models. The solid lines show the implied AGN luminosity function. (More realistic models would keep the AGN luminosity function fixed to the observations by adjusting other parameters, but these simple models are sufficient to illustrate our point.) *Middle*: Distribution of mass for halos that host AGNs with luminosities $10^6 L_{\odot}^{\text{Edd}} < L < 10^8 L_{\odot}^{\text{Edd}}$ and $10^8 L_{\odot}^{\text{Edd}} < L < 10^{10} L_{\odot}^{\text{Edd}}$. Here L_{\odot}^{Edd} is the Eddington luminosity of a $1 M_{\odot}$ black hole. *Bottom*: Derived duty cycle for AGNs in the same luminosity ranges. The duty cycles were estimated by dividing the number of AGNs in the luminosity range by the number density of halos more massive than the mean shown in the middle panels. These panels show that the duty cycle decreases at high luminosities if there is significant scatter in the M_h-L relationship or if black hole accretion is suppressed in the most massive halos. Increases in dust obscuration with luminosity can also reduce the duty cycle at high L , but we judged this effect too obvious to illustrate here.

REFERENCES

- Adelberger, K. L. 2005, *ApJ*, 621, 574
- Adelberger, K. L., Shapley, A. E., Steidel, C. C., Pettini, M., Erb, D. K., & Reddy, N. A. 2005a, *ApJ*, 629, 636
- Adelberger, K. L., & Steidel, C. C. 2000, *ApJ*, 544, 218
- Adelberger, K. L., Steidel, C. C., Giavalisco, M., Dickinson, M., Pettini, M., & Kellogg, M. 1998, *ApJ*, 505, 18
- Adelberger, K. L., Steidel, C. C., Pettini, M., Shapley, A. E., Reddy, N. A., & Erb, D. K. 2005b, *ApJ*, 619, 697
- Adelberger, K. L., Steidel, C. C., Shapley, A. E., Hunt, M. P., Erb, D. K., Reddy, N. A., & Pettini, M. 2004, *ApJ*, 607, 226
- Cristiani, S., & Vio, R. 1990, *A&A*, 227, 385
- Croom, S. M., Smith, R. J., Boyle, B. J., Shanks, T., Miller, L., Outram, P. J., & Loaring, N. S. 2004, *MNRAS*, 349, 1397
- Croom, S. M., et al. 2005, *MNRAS*, 356, 415
- Ferrarese, L. 2002, *ApJ*, 578, 90
- Frenk, C. S., et al. 2000, preprint (astro-ph/0007362)
- Haiman, Z., & Hui, L. 2001, *ApJ*, 547, 27
- Ho, L. C. 2004, in *Coevolution of Black Holes and Galaxies*, ed. L. C. Ho (Cambridge: Cambridge Univ. Press), 293
- Hopkins, P. F., Hernquist, L., Cox, T. J., Di Matteo, T., Martini, P., Robertson, B., & Springel, V. 2005, *ApJ*, in press (astro-ph/0504190)
- Hunt, M. P., Steidel, C. C., Adelberger, K. L., & Shapley, A. E. 2004, *ApJ*, 605, 625
- Jenkins, A., et al. 1998, *ApJ*, 499, 20
- Kaiser, N. 1984, *ApJ*, 284, L9
- Kauffmann, G., Colberg, J. M., Diafero, A., & White, S. D. M. 1999, *MNRAS*, 303, 188
- Kauffmann, G., & Haehnelt, M. G. 2002, *MNRAS*, 332, 529
- Lynden-Bell, D. 1969, *Nature*, 223, 690
- Martini, P. 2004, in *Coevolution of Black Holes and Galaxies*, ed. L. C. Ho (Cambridge: Cambridge Univ. Press), 170
- Martini, P., & Schneider, P. 2003, *ApJ*, 597, L109
- Martini, P., & Weinberg, D. H. 2001, *ApJ*, 547, 12
- Merloni, A. 2004, *MNRAS*, 353, 1035
- Richards, G. T., Vanden Berk, D. E., Reichard, T. A., Hall, P. B., Schneider, D. P., SubbaRao, M., Thakar, A. R., & York, D. G. 2002, *AJ*, 124, 1
- Shapley, A. E., Steidel, C. C., Pettini, M., & Adelberger, K. L. 2003, *ApJ*, 588, 65
- Soltan, A. 1982, *MNRAS*, 200, 115
- Spergel, D. N., et al. 2003, *ApJS*, 148, 175
- Steidel, C. C., Adelberger, K. L., Shapley, A. E., Pettini, M., Dickinson, M., & Giavalisco, M. 2003, *ApJ*, 592, 728
- Steidel, C. C., Hunt, M. P., Shapley, A. E., Adelberger, K. L., Pettini, M., Dickinson, M., & Giavalisco, M. 2002, *ApJ*, 576, 653
- Steidel, C. C., Shapley, A. E., Pettini, M., Adelberger, K. L., Erb, D. K., Reddy, N. A., & Hunt, M. P. 2004, *ApJ*, 604, 534